

Structural Change in Lithium Intercalation of Layered Perovskite $\text{LiLaNb}_2\text{O}_7$

Mineo SATO,* Tetsuro JIN, and Hirokazu UEDA

Department of Chemistry and Chemical Engineering, Faculty of Engineering,
Niigata University, Ikarashi 2-nocho, Niigata 950-21

The chemical lithium intercalation of a layered perovskite $\text{LiLaNb}_2\text{O}_7$ compound has been performed by using *n*-butyllithium. The content of inserted lithium ions was found to be *ca.* 1 mol per unit formula. The crystal structure of the intercalated compound was determined by the powder X-ray diffraction pattern. An unusual contraction of the cell volume inherent in the intercalation reaction was observed.

A series of layered oxides, generally formulated as $\text{M}[\text{A}_{n-1}\text{B}_n\text{O}_{3n+1}]$ (M=alkali, A=alkaline earths or rare earths, B=titanium or niobium), derived from the perovskite structure have attracted much attention.¹⁻⁵⁾ These compounds with interlayer alkali metal cations are closely related to the Ruddlesden-Popper series,⁶⁾ but unlike them readily undergo ion-exchange reactions with alkali molten salts and with aqueous acids. And also their protonated forms are known to behave as strong Brønsted acids, readily intercalating organic bases.^{7,8)} The structures of the exchanged products are in quite analogy to those of the parent materials although the stacking sequence of the perovskite layers are often rearranged in order to optimize the interlayer cation coordination. In sodium and lithium ion-exchanged compounds, *e.g.*, MLaNb_2O_7 (M=Li,Na)⁹⁾ and $\text{NaCa}_2\text{NaNb}_4\text{O}_{13}$,¹⁰⁾ a MO_4 tetrahedral coordination with the central site occupancy equal to 50% occurs as a consequence of the stacking displacement of the adjacent perovskite sheets by 1/2 unit along the diagonal direction of the sheet. These compounds are also known to exhibit an ion conduction due to the interlayer ions, probably having a fairly high mobility for ionic motion within the interlayer.^{1,9)} These facts may lead to the possibility that an appreciable quantity of lithium can be inserted topochemically into the interlayer site with a possible simultaneous reduction of Nb^{5+} to Nb^{4+} . We report here a chemical lithium intercalation of $\text{LiLaNb}_2\text{O}_7$ by using *n*-butyllithium and the crystal structure of the intercalated product determined by the Rietveld method.

$\text{LiLaNb}_2\text{O}_7$ was prepared by an ion-exchange reaction of KLaNb_2O_7 with a large excess amount of a LiNO_3 molten salt in the same way as described previously.⁹⁾ The lithium intercalation reaction was carried out by a chemical lithiation of $\text{LiLaNb}_2\text{O}_7$ powder with an excess of *n*-butyllithium (1.49 mol dm^{-3} in hexane) in a water-free hexane solution at 25 °C for 5 days under a nitrogen atmosphere. After the reaction, the color of the product was changed from white to black. The product was thoroughly washed with hexane, dried at 100 °C under vacuum, and stored in an ampule filled with nitrogen gas. Since the intercalated product did not dissolve in any strong acid solutions, the inserted lithium content was determined by a sort of back titration for lithium ions remaining in the solution after the intercalation reaction. The amount was found to be 1.01 mol per unit formula. Therefore, the intercalated product can be regarded as a stoichiometric compound,

$\text{Li}_2\text{LaNb}_2\text{O}_7$. Powder X-ray diffraction data were collected using $\text{CuK}\alpha$ radiation and a θ - 2θ diffractometer (Rigaku Denki, RAD-rA) with a curved-graphite monochromator located on the diffracted beam side. Since the intercalated compound was slightly oxidized in the ambient atmosphere, the diffraction measurement was performed using a homemade attachment filled with a nitrogen flow atmosphere (100 ml min^{-1}). The counting rate was 4 s at each step of 0.02° over the 2θ range of $10 - 100^\circ$. The structure refinement of the compound was performed using the total pattern fit program RIETAN¹¹⁾ based on the Rietveld method. The crystal structure of $\text{LiLaNb}_2\text{O}_7$ had been determined in the previous work.⁹⁾ The unit cell parameters of the compound are $a=3.8798 \text{ \AA}$, $c=20.3579 \text{ \AA}$ and $Z=2$ for a tetragonal symmetry with $I4/mmm$ space group. The X-ray diffraction peaks found in the intercalated compound were all indexed as the same space group. The Rietveld refinement for the compound was, therefore, performed assuming the same structural model as that of $\text{LiLaNb}_2\text{O}_7$. Structural refinement for $\text{LiLaNb}_2\text{O}_7$ was also made so as to compare the results between the two compounds. A correction on preferred orientation was applied for a plate-like crystal oriented along $[002]$ direction. In the early refinement stage, the site assignment for lithium ions was not included because of its low atomic scattering factor. After several refinement stages, the location of the Li ion site could be assigned by means of the Fourier difference maps. The crystal data and structural parameters finally obtained are summarized in Tables 1 and 2. Figure 1 shows the final best-fit profiles obtained

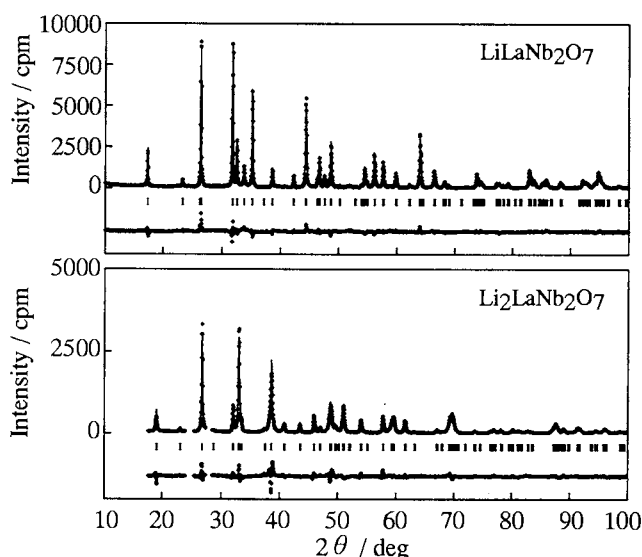


Fig.1. X-ray diffraction pattern fitting for $\text{Li}_{1+x}\text{LaNb}_2\text{O}_7$ ($x=0,1$). The calculated and observed data are shown as solid lines and dots. The vertical marks show positions of Bragg reflections. The trace is a plot of the difference between calculated and observed data.

Table 1. Data-collection conditions, crystallographic data, and reliable factors for $\text{LiLaNb}_2\text{O}_7$ and $\text{Li}_2\text{LaNb}_2\text{O}_7$

	$\text{LiLaNb}_2\text{O}_7$	$\text{Li}_2\text{LaNb}_2\text{O}_7$
Radiation	$\text{CuK}\alpha$	$\text{CuK}\alpha$
2θ range ($^\circ$)	10-100	10-100
Step scan 2θ increment ($^\circ$)	0.02	0.02
Count time (sec step ⁻¹)	4	4
Space group	$I4/mmm$	$I4/mmm$
a (\AA)	3.8799(1)	3.9409(3)
c (\AA)	20.3606(5)	18.633(1)
Volume (\AA^3)	306.5	289.3
Z	2	2
Calculated density (g cm^{-3})	4.807	5.171
No. of parameters refined	27	27
Reliable factors ^{a)}		
R_{wp}	0.1247	0.1657
R_{p}	0.0898	0.1279
R_{I}	0.0467	0.0493
R_{F}	0.0302	0.0213

a) Defined in Ref.11.

Table 2. Positional parameters for $\text{LiLaNb}_2\text{O}_7$ and $\text{Li}_2\text{LaNb}_2\text{O}_7$

Phase	Atom	Site	g	x	y	z	$B/\text{\AA}^2$
$\text{LiLaNb}_2\text{O}_7$	Li	4d	0.5	0.0	0.5	0.25	6.4(6)
	La	2a	1.0	0.0	0.0	0.0	0.3(2)
	Nb	4e	1.0	0.0	0.0	0.3889(2)	0.1(1)
	O(1)	8g	1.0	0.0	0.5	0.0894(15)	2.8(10)
	O(2)	4e	1.0	0.0	0.0	0.3044(20)	3.9(12)
	O(3)	2b	1.0	0.0	0.0	0.5	1.7(17)
$\text{Li}_2\text{LaNb}_2\text{O}_7$	Li	4d	1.0	0.0	0.5	0.25	2.2(11)
	La	2a	1.0	0.0	0.0	0.0	0.3(2)
	Nb	4e	1.0	0.0	0.0	0.3852(4)	0.3(3)
	O(1)	8g	1.0	0.0	0.5	0.0972(20)	0.7(20)
	O(2)	4e	1.0	0.0	0.0	0.2847(20)	1.2(14)
	O(3)	2b	1.0	0.0	0.0	0.5	0.1(20)

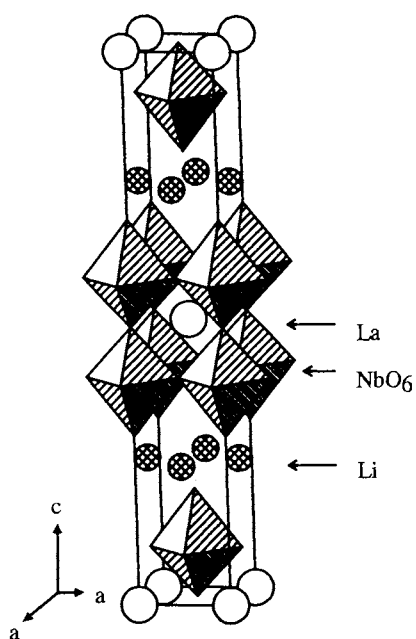


Fig. 2. Crystal structure of $\text{Li}_{1+x}\text{LaNb}_2\text{O}_7$.

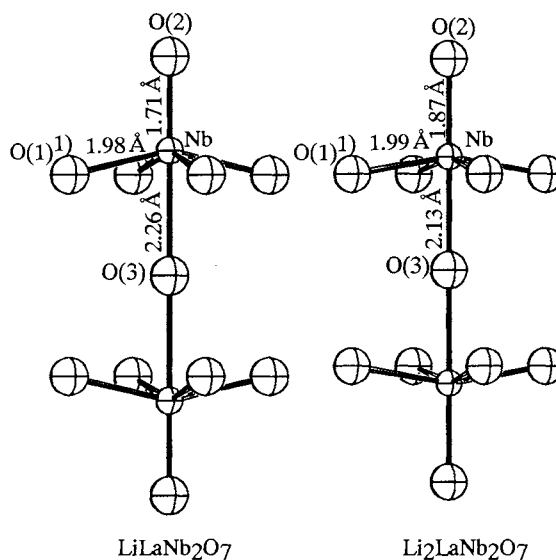


Fig. 3. Environment around Nb atoms in $\text{Li}_{1+x}\text{LaNb}_2\text{O}_7$.

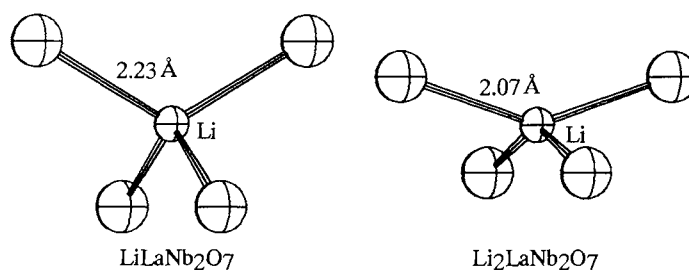


Fig. 4. Environment around Li atoms in $\text{Li}_{1+x}\text{LaNb}_2\text{O}_7$.

by the refinement together with the raw data. Relatively high R -factors are achieved in the case of $\text{Li}_2\text{LaNb}_2\text{O}_7$. This may be due to the fact of the poor crystallinity occurring during the intercalation reaction, as shown in Fig. 1. Particularly, the threshold of diffraction peaks at low 2θ region fades out gradually toward the low side of angle, giving a significant asymmetric peak profile. The cell and positional parameters obtained for $\text{LiLaNb}_2\text{O}_7$ are quite similar to those in the previous study,⁹⁾ virtually regarded as the same results. The two compounds have the same type crystal structure (Fig. 2). The structure comprises perovskite-like layers of NbO_6 octahedra that are terminated along one of the perovskite cubic directions. The layers are two octahedra thick and contain lanthanum cations which are located at the site corresponding to the A site of an ideal perovskite. With the lithium intercalation reaction, the a axis increases while the c axis decreases, totally resulting overall contraction of the unit cell volume. Such a contraction seems to be quite unusual in typical lithium intercalation reactions found in transition disulfides,¹²⁾ MoO_3 ,¹²⁾ Fe_3O_4 ¹³⁾ and so on, where the lithium insertion into the host always results in an increase in the cell volume. Figure 3 shows the environment around niobium atoms in the perovskite unit. There are three kinds of Nb–O bond distances in a NbO_6 octahedron; a considerably shortened bond (1.71 Å), two normal bonds (1.98 Å) and a long bond

(2.26 Å), the average Nb–O bond distance being 1.98 Å. These bond character can be seen in other layered perovskite oxides and their ion-exchanged products. Since the ion-exchangeable layered perovskite have less charge density compared with the Ruddlesden–Popper phases,²⁾ it can be considered that the niobium cation located in the center of the octahedron moves toward the interlayer side so as to compensate the less charge density of the interlayer space. On the other hand, the shortened bond and the long bond increase and decrease, respectively, in $\text{Li}_2\text{LaNb}_2\text{O}_7$ although three kinds of bond distances still exist (the average Nb–O bond distance, 2.00 Å). That is, the NbO_6 octahedron becomes less distorted and close to an ideal octahedron accompanied by the lithium intercalation. These facts are reasonably interpreted that the less charge density present in the interlayer space of $\text{LiLaNb}_2\text{O}_7$ is canceled in some extent by the lithium insertion into the interlayer site which is already occupied by the lithium ions with 50% site occupancy. The increase in the average Nb–O bond distance found in $\text{Li}_2\text{LaNb}_2\text{O}_7$ may be due to the reduction from Nb^{5+} to Nb^{4+} . Figure 4 shows the environment around lithium atoms. In $\text{NaLaNb}_2\text{O}_7$ which crystallizes the same structure, the NaO_4 tetrahedron is almost regular. However, the LiO_4 tetrahedron in $\text{LiLaNb}_2\text{O}_7$ is fairly distorted from an ideal one as shown in Fig.4, probably because of too small ionic radius of lithium. This tetrahedron becomes quite deformed after the lithium intercalation, coming close to a square-planar coordination. The distance of Li–O bond in the LiO_4 tetrahedron changes from 2.23 to 2.07 Å inherent in the intercalation, becoming closer to the sum of their effective ionic radii, 1.94 Å (Li (IV) 0.59 Å, O (II) 1.35 Å).¹⁴⁾ The considerably compressed LiO_4 tetrahedron may be originated by the increase in the coulomb interaction between the perovskite layers and the lithium site, the positive charge density of which becomes twice as a consequence of the lithium insertion into the site. This is also the origin of the contraction of the *c* axis in $\text{Li}_2\text{LaNb}_2\text{O}_7$.

References

- 1) M. Dion, M. Ganne, and M. Tournoux, *Mat. Res. Bull.*, **16**, 1429(1981).
- 2) A. J. Jacobson, J. W. Johnson, and J. T. Lewandowski, *Inorg. Chem.*, **24**, 3727(1985).
- 3) M. Gondrand and J.-C. Joubert, *Rev. Chim. Miner.*, **24**, 33(1987).
- 4) J. Goparakrishnan and V. Bhat, *Inorg. Chem.*, **26**, 4299(1987).
- 5) J. Goparakrishnan, V. Bhat, and B. Raveau, *Mat. Res. Bull.*, **22**, 413(1987).
- 6) S. N. Ruddlesden and P. Popper, *Acta Cryst.*, **11**, 45(1958).
- 7) A. J. Jacobson, J. T. Lewandowski, and J. W. Johnson, *Mat. Res. Bull.*, **25**, 679(1990).
- 8) R. A. M. Ram and A. Clearfield, *J. Solid State Chem.*, **94**, 45(1991).
- 9) M. Sato, J. Abo, T. Jin, and M. Ohta, *J. Alloys Comp.*, **192**, 81(1993).
- 10) M. Sato, Y. Kono, and T. Jin, *J. Ceram. Soc. Jpn.*, **101**, 980(1993).
- 11) F. Izumi, *Nippon Kessho Gakkaishi*, **27**, 23(1978).
- 12) M. S. Whittingham, *Prog. Solid State Chem.*, **12**, 41(1978).
- 13) M. S. Islam and C. R. A. Catlow, *J. Solid State Chem.*, **77**, 180(1988).
- 14) R. D. Shannon, *Acta Cryst.*, **A32**, 751(1976).

(Received October 6, 1993)